Localization of the discontinous immunodominant region recognized by human anti-thyroperoxidase autoantibodies in autoimmune thyroid diseases

Damien Bresson, Martine Cerutti, Gerard Devauchelle, Martine Pugnière, Françoise Roquet, Cédric Bès, Carine Bossard, Thierry Chardès, Sylvie Péraldi-Roux

THE JOURNAL OF BIOLOGICAL CHEMISTRY
Vol. 278, No. 11, Issue of March 14, pp. 9560–9569, 2003

Printed in U.S.A.

Localization of the Discontinuous Immunodominant Region Recognized by Human Anti-thyroperoxidase Autoantibodies in Autoimmune Thyroid Diseases*

Received for publication, November 22, 2002, and in revised form, December 23, 2002
Published, JBC Papers in Press, December 24, 2002, DOI 10.1074/jbc.M211930200

Damien Bresson‡§, Martine Cerutti¶, Gérard Devauchelle¶, Martine Pugnière‡, Françoise Roquet‡, Cédric Bès‡‖, Carine Bossard‡‡, Thierry Chardès¶, and Sylvie Péraldi-Roux‡**

*From the ‡CNRS Unité Mixte de Recherche (UMR) 5094, Faculté de Pharmacie, 15 avenue Charles Flahault, B. P. 14491, Montpellier 34093 Cedex 5, ¶CNRS-Institut National de la Recherche Agronomique UMR 5087, Station de Recherche de Pathologie Comparée, St. Christol-lez-Alès 30380, and **INSERM U397, Institut Fédératif de Recherche Louis Bugnard, Centre Hospitalier Universitaire Rangueil, Toulouse 31403 Cedex 4, France*

The discontinuous immunodominant region (IDR) recognized by autoantibodies directed against the thyroperoxidase (TPO) molecule, a major autoantigen in autoimmune thyroid diseases, has not yet been completely localized. By using peptide phage-displayed technology, we identified three critical motifs, L*X*PE*X*D, QSYP, and E*X*(E/D)PPV, within selected mimotopes which interacted with the human recombinant anti-TPO autoantibody (aAb) T13, derived from an antibody phage-displayed library obtained from thyroid-infiltrating TPO-selected B cells of Graves' disease patients. Mimotope sequence alignment on the TPO molecule, together with the binding analysis of the T13 aAb on TPO mutants expressed by Chinese hamster ovary cells, demonstrated that regions 353–363, 377–386, and 713–720 from the myeloperoxidase-like domain and region 766–775 from the complement control protein-like domain are a part of the IDR recognized by the recombinant aAb T13. Furthermore, we demonstrated that these regions were involved in the binding to TPO of sera containing TPO-specific autoantibodies from patients suffering from Hashimoto's and Graves' autoimmune diseases. Identification of the IDR could lead to improved diagnosis of thyroid autoimmune diseases by engineering "mini-TPO" as a target autoantigen or designing therapeutic peptides able to block undesired autoimmune responses.

Human thyroid peroxidase (TPO),[1] described previously as the "thyroid microsomal antigen" (1), is a membrane-bound enzyme expressed at the apical pole of thyrocytes (2). TPO generates the functional form of thyroglobulin by iodination and coupling of tyrosine residues (3). During autoimmune thyroid diseases (AITD), TPO represents a major target for the immune system (4, 5), leading to high titer TPO-specific autoantibodies (aAbs) in the sera of patients suffering from Hashimoto's thyroiditis and Graves' disease. Besides their role as efficient and early diagnostic markers of AITD, TPO-specific aAbs also act as effector molecules either through modulating antigen presentation to T cells or by mediating thyroid destruction after complement activation or antibody-dependent cell cytotoxicity (6–12). Alignment studies and structural homologies have shown that TPO is formed by three distinct domains: a myeloperoxidase (MPO)-like, a complement control protein (CCP)-like, and an EGF-like domain, from the N- to the C-terminal extremities (13). Although the structure of each domain has been elucidated in part by three-dimensional modeling (13–16), the full three-dimensional structure of TPO remains unknown, even though low resolution crystals have been obtained (17, 18). The flexibility observed for the hinge regions probably make difficult the exact positioning of each domain in relation to the others (15).

These observations denote a highly complex structure of TPO, thus explaining the reason why TPO aAbs from patients' sera preferentially recognize discontinuous epitopes on TPO (19–22). Different approaches have been used to determine the epitopic regions recognized by anti-TPO aAbs from patients' sera as well as critical amino acids involved in these interactions: (i) competition for TPO binding between mouse mAbs or rabbit polyclonal antisera and human anti-TPO aAbs (13, 23–25), (ii) analysis of human anti-TPO aAb binding to recombinant and/or truncated antigen (15, 16, 26–30), (iii) generation of TPO fragments by enzymatic hydrolysis following by analysis of their binding to TPO aAbs (31, 32), and (iv) eukaryotic cell expression of chimeric MPO-TPO proteins obtained by "guided" mutagenesis and binding analysis to TPO aAbs (33–35). These approaches have demonstrated a restricted response of TPO-specific aAbs, which mainly recognize a discontinuous immunodominant region (IDR). By competition between human anti-TPO from patients' sera and a pool of murine anti-TPO mAbs, the IDR was divided into two overlapping domains named A and B (25). Using monoclonal human anti-TPO antibody fragments (Fabs) as competitor, Chazenbalk and co-workers (23) defined the A and B domains but inverted the nomenclature. This second nomenclature, defined by the human Fabs, will be used here. The IDR was only partially characterized, however, with no clear direct relation between the identified regions. We hypothesize that most of the techniques currently

* The costs of publication of this article were defrayed in part by the payment of page charges. This article must therefore be hereby marked "*advertisement*" in accordance with 18 U.S.C. Section 1734 solely to indicate this fact.

§ Recipient of a fellowship from the CNRS and the Région Languedoc-Roussillon. To whom correspondence should be addressed. Tel.: 33-467-548-609; Fax: 33-467-548-610; E-mail: damienbresson@yahoo.fr.

‖ Supported by the Agence National de Recherche contre le Sida.
‡‡ Supported by the Association pour la Recherche contre le Cancer.

[1] The abbreviations used are: TPO, thyroid peroxidase; aAb, autoantibody; AITD, autoimmune thyroid disease(s); CCP, complement control protein; CHO, Chinese hamster ovary; EGF, epidermal growth factor; ELISA, enzyme-linked immunosorbent assay; hTPO, human TPO; IBS, immunodominant binding surface; IDR, immunodominant region; mAb, monoclonal antibody; MPO, myeloperoxidase; PBS, phosphate-buffered saline; wt, wild-type.

TABLE I
Description of sera from patients suffering from autoimmune thyroid diseases
TSH, thyroid-stimulating hormone; T_3, triiodothyronine; T_4, thyroxine; TRAK, TSH receptor autoantibodies.

Patient no.	Disease	TPO autoantibody titer[a]	TSH	T_3	T_4	TRAK[b]
		units/ml	*microunits/ml*	*pg/ml*	*ng/dl*	*units/liter*
1	Hashimoto	9,309	11.84	2.13	0.98	ND[c]
2	Hashimoto	3,141	32.20	2.38	0.95	ND
3	Hashimoto	7,148	16.05	1.85	1.59	ND
4	Hashimoto	23,867	14.80	1.60	ND	ND
5	Hashimoto	3,141	0.01	3.74	3.15	ND
6	Graves	2,242	6.02	2.85	17.20	ND
7	Graves	4,633	6.00	2.60	ND	19.00
8	Graves	3,793	0.01	16.20	2.00	13.50
9	Graves	1,426	2.82	ND	ND	ND
10	Graves	1,443	0.01	1.40	ND	1.15
Normal values		<140	0.10–3.50	0.85–3.00	0.90–3.00	<1.50

[a] The values were obtained by radioimmunoassay and standardized to the WHO/National Institute for Biological Standards and Control 66/387 (see "Experimental Procedures").
[b] The values were obtained by a radio receptor assay using a DYNOtest TRAK human kit and standardized to the WHO 90/672 (see "Experimental Procedures").
[c] ND, not determined.

in use for mapping mAb linear epitopes are inadequate for precisely defining a discontinuous epitope on molecules like TPO, which have a highly organized architecture. To overcome this problem, we decided to combine two technological advances already used to delineate highly structured epitopes (36–39). First, antibody-specific peptides were selected for their ability to mimic natural epitopes by screening phage-displayed peptides libraries. Second, the sequence alignments of such selected mimotopes on the primary sequence of the antigen together with knowledge of the three-dimensional structure of the antigen allowed the identification of a potential conformational epitope.

We applied this strategy to the identification of the TPO immunodominant epitope involved in thyroid autoimmunity by using the human IDR-specific recombinant IgG_1 aAb T13 derived from antibody phage-displayed libraries obtained from B cells extracted from thyroid tissue of Graves' disease patients (40, 41). Four distinct regions, belonging to the MPO-like and CCP-like domains of TPO, delimited the discontinuous IDR, recognized by the human recombinant aAb T13 and identified by sera from patients suffering from Hashimoto's thyroiditis or Graves' disease.

EXPERIMENTAL PROCEDURES

Patient Sera—Sera from five patients with Graves' disease, five with Hashimoto's thyroiditis, and four healthy donors were obtained from Dr. L. Baldet and Dr. A. M. Puech (Guy de Chauliac Hospital, Montpellier, France). The anti-TPO aAb titers were determined by radioimmunoassay using the TPO-AB-CT Kit (Cis bio, Gif sur Yvette, France). The patients' sera were characterized further for the presence of anti-TSH receptor aAbs by a radio receptor assay using the TRAK human kit (BRAHMS, Hennigsdorf, Germany) and for triiodothyronine, thyroxine, and thyroid-stimulating hormone levels (Table I). As controls, sera from eight patients suffering from other autoimmune affections, two with type 1 diabetes, four with human systemic lupus erythematosus, one with vascularitis, and one with rheumatoid arthritis were tested.

Materials—The human TPO (hTPO), purified (greater than 95% pure) from thyroid glands, was obtained from HyTest Ltd. (Turku, Finland). The plasmid encoding full-length hTPO was kindly provided by Dr. B. Rapoport (Cedars-Sinai Medical Center, Los Angeles, CA). Anti-TPO mAb 47 was provided by Dr. J. Ruf (INSERM Unit 555, Marseille, France) (42). Anti-TPO mAb 6F5 and rabbit polyclonal anti-TPO were purchased from HyTest Ltd., and Abcys S.A. (Paris, France), respectively.

Cloning, Expression, and Purification of Human aAb T13—The recombinant human anti-TPO scFv T13 was selected from an antibody phage-displayed library obtained from B cells extracted from thyroid tissue of Graves' disease patients (40). The T13 aAb was expressed as an entire IgG_1 antibody by using the baculovirus/insect cell system as described (41, 43, 44). IgG_1 T13 was purified on a protein G affinity column and the concentration determined by the $A_{280\ nm}$, $E^{0.1\%}$ of 1.40.

Purity, Specificity, and Kinetic Parameters of aAb T13—The purity was analyzed on 8% SDS-PAGE under nonreducing conditions, then Coomassie Brilliant Blue stained or transferred to a polyvinylidene difluoride membrane (Novex, San Diego), and revealed by a peroxidase-conjugated anti-human IgG Fc-specific Ab (Sigma) diluted 1:1,000, using the ECL detection system (Amersham Biosciences). Then, the aAb specificity was determined by ELISA. The microtiter plate wells were coated with 9 nM (1 μg/ml) TPO in 100 mM $NaHCO_3$, pH 9, overnight at 4 °C. Plates were washed with 0.05% Tween 20 in PBS (PBS-T), pH 7.3, and blocked with 2% powdered milk in PBS-T for 1 h at 37 °C. After washing, aAb T13 or purified human IgG_1 (Sigma) as control was incubated with 1% powdered milk in PBS-T (incubation buffer) for 1.5 h at 37 °C. After washing, an alkaline phosphatase-conjugated anti-human IgG Ab (Sigma, diluted 1:1,000) in the incubation buffer was added, and the plates were incubated for 1 h at 37 °C. After three washings, the reactivity was revealed with 1 mg/ml of 4-nitrophenyl phosphate in 0.5 M diethanolamine/HCl, pH 9.6, for 1 h at 37 °C. Kinetic parameters of aAb T13 were obtained by real time analysis as described previously (41). The aAb T13, expressed as scFv or IgG_1, inhibits between 7.3 and 100% of the binding to TPO of serum samples from patients with AITD that were tested (40, 41).

Panning and Screening of Phage-displayed Peptides—Four phage-displayed libraries (LX-8/f88.4, X_{15}/f88.4, X_8CX_8/f88.4, and X_{30}/f88.4) in which peptides were displayed at the N terminus of the pVIII coat protein on the surface of the filamentous bacteriophage M13, were obtained from Dr. J. Scott (Simon Fraser University, Burnaby, Canada) (45). Phages specific for aAb T13 were selected by biopanning as described previously (46). Antibody-bound phages were eluted (i) by 3 ml of acid elution (0.1 M glycine-HCl (pH 2.2), 1 mg/ml bovine serum albumin) for 30 min at room temperature and further neutralization by adding 300 μl of 2 M Tris/HCl, pH 9.2; (ii) by competition with a 180 nM (20 μg/ml) TPO solution in 5 ml of NaCl/Tris (50 mM Tris, 150 mM NaCl, 0.05% Tween 20, pH 7.5) for 2 h at 37 °C. Phages were amplified after each round of panning using an exponentially growing culture of *Escherichia coli* K91 cells, and T13-specific phages were cloned and characterized by ELISA as described (46). Clones giving an absorbance more than twice the background level were selected.

Each selected and purified clone was checked further by ELISA for its ability to be inhibited by soluble TPO at a concentration of 90 nM (10 μg/ml). Briefly, wells from microtiter plates were coated with 13 nM aAb T13 in 100 mM $NaHCO_3$, pH 9, overnight at 4 °C. Plates were washed with PBS-T, and then 2% powdered milk in PBS-T was added for 1 h at 37 °C. After saturation and four washings, a 1:10 dilution of purified phages from each clone was coincubated with soluble TPO for 1.5 h at 37 °C. After washing, a horseradish peroxidase-conjugated anti-M13 (Amersham Biosciences; diluted 1:5,000 with 1% powdered milk in PBS-T) was added for 1 h at 37 °C. Three washings were performed, and residual bound phages were revealed with 4 mg/ml 2-phenylenediamine solution containing 0.03% (v/v) hydrogen peroxide in 0.1 M citrate

buffer, pH 5.0. After 20 min, the reaction was stopped by adding 50 μl of 2 M H_2SO_4 to each well, and the resulting absorbance was measured at 490 nm. Selected phages, whose binding to aAb T13 was inhibited by more than 15%, were sequenced for peptide sequence identification. As a control, the effect of a solution containing 90 nM soluble thyroglobulin (60 μg/ml) on the binding of these selected phages to aAb T13 was tested.

Mimotope Synthesis, Alanine Scanning, and Immunoassay on Cellulose Membrane-bound Peptides—The general protocol of Spot parallel peptide synthesis has been described previously (47). 12 pentadecapeptides corresponding to the selected T13-specific mimotopes and their 15 alanine analogs were synthesized by the Spot method. The membrane-bound peptides were probed by coincubation of a 0.1 μM solution of aAb T13 with peroxidase-conjugated anti-human Fc specific antibody (Sigma) diluted 1:1,000 for 1.5 h at 37 °C. After three washings, the complex was revealed using the ECL detection system on a sensitive film, and the intensities of the spots were evaluated with ScionImage software. The membrane was reused after a regeneration cycle.

Sequence Alignments and Molecular Modeling—Each amino acid sequence corresponding to an immunoreactive mimotope was aligned with the other selected peptides or with the hTPO sequence using the multiple sequence alignment program Multalin (48). The sequence homologies between T13-specific mimotopes and hTPO were located on a three-dimensional model of TPO, using the atomic coordinates kindly provided by Hobby *et al.* (13).

Directed Mutagenesis and Stable Expression of Wild-type and Mutated TPO cDNA—A *Kpn*I restriction site was added by PCR just after the stop codon of the full-length hTPO cDNA. Wild-type TPO cDNA was cloned using the *Hin*dIII and *Kpn*I sites into the pcDNA5/FRT expression vector from the Flp-In system (Invitrogen). The mutants were constructed by overlap extension PCR as described previously (49). The mutation replacements were performed as follows. The ^{353}HARLRDSGRAY^{363} sequence from wt TPO was replaced by sequence ^{353}NQAFQANGAAL^{363} in the TPO$^{353-363}$ mutant, wt TPO (^{377}PEPGIPGETR^{386}) by TPO$^{377-386}$ (^{377}LLTNRLGRIG^{386}), wt TPO (^{506}ASFQEHPDL^{514}) by TPO$^{506-514}$ (^{506}NRYLPMEPN^{514}), wt TPO (^{713}KFPEDFES^{720}) by TPO$^{713-720}$ (^{713}SYARLAVN^{720}), wt TPO (^{737}PQDD^{740}) by TPO$^{737-740}$ (^{737}ALAA^{740}), and wt TPO (^{766}YSCRHGYELQ^{775}) by TPO$^{766-775}$ (^{766}LTCEGGFRIS^{775}). All sequences were verified by the dideoxynucleotide termination method (50). The Flp-In system was used to generate isogenic stable mammalian cell lines expressing wt and mutated TPO. CHO cells (ATCC CCL61) were routinely grown in Dulbecco's modified Eagle's medium/nutrient mixture F-12 containing 10% fetal calf serum. Stable transfectants were obtained as recommended by the manufacturer. Briefly, the CHO host cell line was constructed by transfection with 0.5 μg of the pFRT/*lac*Zeo vector and selection with growth medium containing 500 μg/ml Zeocin™ (Cayla, Toulouse, France). Zeocin™-resistant clones were screened to identify those containing a single integrated FRT site and expressing a high β-galactosidase level. A single clone was selected and amplified for further studies. The generation of wt or mutated TPO was obtained by cotransfection, into the selected Zeocin™-resistant CHO host cell line, of the hygromycin-resistant pcDNA5/FRT plasmids bearing each form of TPO and the pOG44 plasmid which constitutively expresses the Flp recombinase. Two days later, the cells were fed with growth medium supplemented with 300 μg/ml hygromycin B (Invitrogen). The clones of interest were selected for hygromycin resistance, Zeocin™ sensitivity, and lack of β-galactosidase activity.

Membrane Protein Extraction—Stably transfected CHO cells were washed three times with PBS and scraped at 4 °C. Membrane protein extraction was performed as follows. After centrifugation at 1,000 rpm for 5 min at 4 °C, membrane proteins were solubilized by adding 500 μl of lysis buffer (50 mM Tris/HCl, pH 7.3, 150 mM NaCl, 5 mM EDTA, 10% glycerol, 1% Triton X-100, and a protease inhibitor mixture tablet/10 ml of lysis buffer (Roche Molecular Biochemicals)) and incubated for 30 min on ice. After centrifugation at 13,000 rpm for 30 min at 4 °C, the supernatants containing membrane proteins were recovered and conserved at −80 °C. The protein concentrations were evaluated by the BCA protein assay reagent (Pierce).

Western Blotting Analysis and Competition Experiments—Approximately 20 μg of membrane proteins was mixed with protein buffer (0.2 mM Tris/HCl, pH 6.8, 50% glycerol, 1% SDS, and 0.1% bromphenol blue) for native conditions, supplemented with 10% dithiothreitol, 10% 2-mercaptoethanol, and boiled 5 min for denaturing conditions. Each sample was loaded into individual wells and electrophoresed through a 9% SDS-PAGE. Proteins were transferred to nitrocellulose membranes, which were then saturated with 5% powdered milk in PBS-T for 30 min at room temperature. The first antibodies, diluted with the incubation buffer, were applied overnight at 4 °C. After three washings with PBS-T for 10 min at room temperature, the membranes were incubated with horseradish peroxidase-conjugated secondary antibodies diluted in incubation buffer for 1 h at 37 °C. After three washings, the signal was detected with chemiluminescence ECL on a sensitive film.

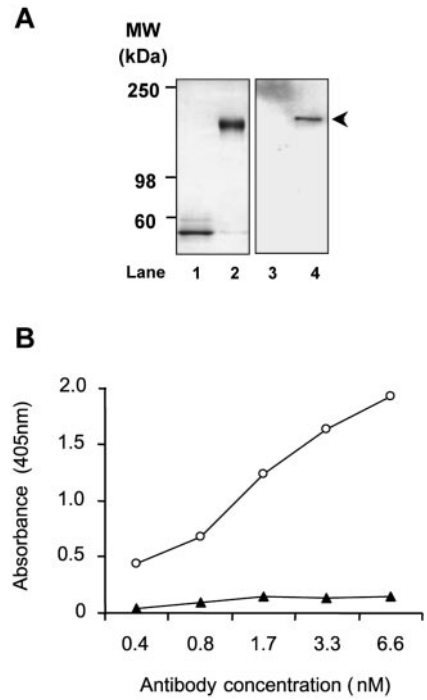

FIG. 1. **Purity and specificity of aAb T13.** Purity and specificity were studied as described under "Experimental Procedures." *A*, each sample (2 μg of proteins) was charged on two 8% polyacrylamide-SDS gels. The first was stained with Coomassie Brilliant Blue R-250 (*lanes 1* and *2*) and the second analyzed by Western blotting (*lanes 3* and *4*). *Lanes 1* and *3* show the baculovirus supernatant before purification. *Lanes 2* and *4* show the aAb T13 after purification (*black arrow*). The molecular masses (*MW*) in kDa are shown on the *left* of the figure. *B*, the specificity of aAb T13 was analyzed by ELISA. The binding of aAb T13 (*open circles*) and human polyclonal IgG_1 as control (*closed triangles*) on TPO is shown.

Competitive ELISA experiments were performed as follows. Briefly, the wells were coated with 9 nM (1 μg/ml) TPO in 100 mM $NaHCO_3$, pH 9, overnight at 4 °C. Then they were washed and blocked with 2% bovine serum albumin in PBS-T (saturation buffer) for 1 h at 37 °C. After three washings, 3 nM mAb T13 (at a dilution giving an A_{490} of 1.5) was incubated with or without decreasing concentrations of inhibitor in saturation buffer for 1.5 h at 37 °C under mild shaking. The wells were washed, and horseradish peroxidase-conjugated anti-human IgG antibody diluted 1:2,000 in saturation buffer was added for 1 h at 37 °C. Three washings were performed, and then aAb T13 bound to TPO was detected by adding 4 mg/ml 2-phenylenediamine solution containing 0.03% (v/v) hydrogen peroxide in 0.1 M citrate buffer, pH 5.0. The reaction was stopped with 2 M H_2SO_4, and the resulting absorbance was measured at 490 nm.

ELISA with mAbs and Human Sera—Wells were coated with 20 μg/ml membrane proteins in PBS overnight at 4 °C. The plates were washed with PBS-T and blocked with the saturation buffer for 1 h at 37 °C. After three washings, mAb or serum was incubated in the saturation buffer for 1.5 h at 37 °C. The plates were washed, and horseradish peroxidase-conjugated anti-human IgG or anti-mouse antibody (diluted 1:2,000 in saturation buffer) was added for 1 h at 37 °C. Three washings were performed, and the reactivity was revealed as described above.

RESULTS

Characterization of aAb T13 Expressed as Whole IgG_1 in Insect Cells—The anti-TPO aAb T13 was first produced in the form of a human scFv (40). For the present study, we produced the entire human IgG_1 T13 by using the baculovirus/insect cell system and purified it by protein G affinity chromatography. The purity was analyzed on 10% SDS-PAGE stained with Coo-

TABLE II
Kinetic parameters of aAb T13 as assessed by real time analysis

Antibody	TPO concentration	Binding[a]	k_a	k_d	K_D (k_d/k_a ratio)
	nM	*RU*	$M^{-1}\ s^{-1} \times 10^5$	$s^{-1} \times 10^{-3}$	*nM*
T13	45	72.0	1.30	0.14	1.09
	90	91.9	2.61	0.18	0.68
	180	106.0	1.64	0.16	0.98
Control	180	ND[b]	NM[c]	NM	NM

[a] The binding of human purified TPO to monoclonal antibodies was measured in resonance units (RU) as described (41). RU values were corrected by subtracting the base line.
[b] ND, not determined.
[c] NM, not measurable.

TABLE III
Peptide sequences selected by phage-displayed peptide library

Elution procedure and no. of clones[a]	Sequence	Absorbance[b] (490 nm)	Inhibition[c]
			%
Acid			
1	KLLPEDDESRTYHTV	1.32	19
2	RLAPEPDDPITPMTK	1.25 ± 0.06[d]	22 ± 3
1	TQSYPPPPAWRAASR	2.11	53
1	QLSPESDYDDHGMRY	3.00	40
1	KLFPEEDEMRTETQR	1.60	24
1	SQSYPEPARGSVPMP	3.00	29
Competition			
1	GQSYPPRPDTSLHVT	0.50	28
1	ELNPEPDTEVFPMTF	0.91	38
1	KNSRQSYPEPAPVYH	0.59	28
1	ENEPPVWTTESKLQS	0.74	31
1	ESDPPVASYQWRLIN	0.79	36
1	ESVMQSYPPHLQIPG	0.50	24

[a] Clones with the same sequence.
[b] Absorbance corresponding to the binding of each clone to aAb T13.
[c] The binding of each clone to aAb T13 was inhibited by soluble human TPO or thyroglobulin at 90 nM; only clones showing an inhibition greater than 15% with hTPO are indicated; no inhibition was observed with thyroglobulin as inhibitor.
[d] When a clone was represented at least twice, the absorbance and percent inhibition values are given as the mean value ± S.D.

TABLE IV
Classification of mimotopes by sequence homology

Family 1	Family 2	Family 3
QLSPESDYDDHGMRY	KNS–RQSYPEPAPVYH	ENEPPVWTTESKLQS
KLLPEDDESRTYHTV	S– –QSYPEPARGSVPMP	ESDPPVASYQWRLIN
KLFPEEDEMRTETQR	T– –QSYP–PPPAWRAASR	
RLAPEPDDPITPMTK	GQSYP–PRPDTSLHVT	
ELNPEPDTEVFPMTF	ESVMQSYP–PHLQIPG	

massie Brilliant Blue under nonreducing conditions (Fig. 1*A*, *left panel*). We visualized a 150 kDa band corresponding to human IgG_1 T13, and the purity was estimated to be superior to 95%. The identity of the band was confirmed by Western blotting, under nonreducing conditions, with a peroxidase-conjugated anti-human IgG Fc-specific Ab (Fig. 1*A*, *right panel*). Approximately 5 mg of purified aAb T13 was obtained per liter of Sf9 insect cell culture supernatant. The binding specificity of aAb T13 to hTPO was determined by ELISA. As shown in Fig. 1*B*, aAb T13 specifically bound hTPO in a dose-dependent manner, whereas polyclonal human IgG_1 as control did not. Moreover, no binding was observed for aAb T13 to thyroglobulin (data not shown).

The kinetic parameters of aAb T13 were assessed by real time analysis, using a BIACORE 2000 as described previously (41), by injecting three concentrations of purified hTPO on aAb T13 or irrelevant Ab (Table II). We found that aAb T13 showed a high affinity for hTPO (K_D = 0.9 nM, average of three experiments) with a low dissociation rate (k_d = 1.6 10^{-4} s^{-1}, average of three experiments), whereas hTPO did not bind to the irrelevant Ab.

Selection of T13-binding Mimotopes by Phage Display Technology—We have demonstrated previously that aAb T13 strongly inhibits the TPO binding of aAb in the sera of patients suffering from AITD (40, 41). Moreover, we have shown that aAb T13 does not recognize a linear epitope,[2] thus suggesting the conformational nature of this dominant cognate epitope. To address this question, biopannings were performed with a mix of four phage libraries expressing peptides with 8, 15, 17, or 30 amino acids at their surface, to obtain specific mimotopes selected by human aAb T13, which mimic the conformational epitope. 100 phages were eluted with a pH 2.2 buffer after three rounds of panning on aAb T13 and another 100 phages after four rounds of panning for the elution by competition. All 200 phages were isolated and then purified. As shown in Table III, 12 T13-specific mimotopes, 6 obtained by acid elution and 6 by competition, were further selected according to (i) their binding level on aAb T13 by ELISA and (ii) their ability to compete with human soluble TPO as inhibitor for aAb T13 binding; only mimotopes with at least 15% inhibition are shown. This inhibition ranging from 19 and 55% for the selected mimotopes. The binding of these mimotopes to the aAb T13 was not inhibited by thyroglobulin, used as a control protein (data not shown). Only peptides derived from

[2] D. Bresson, M. Cerutti, G. Devauchelle, M. Pugnière, F. Roquet, C. Bès, C. Bossard, T. Chardès, and S. Péraldi-Roux, unpublished data.

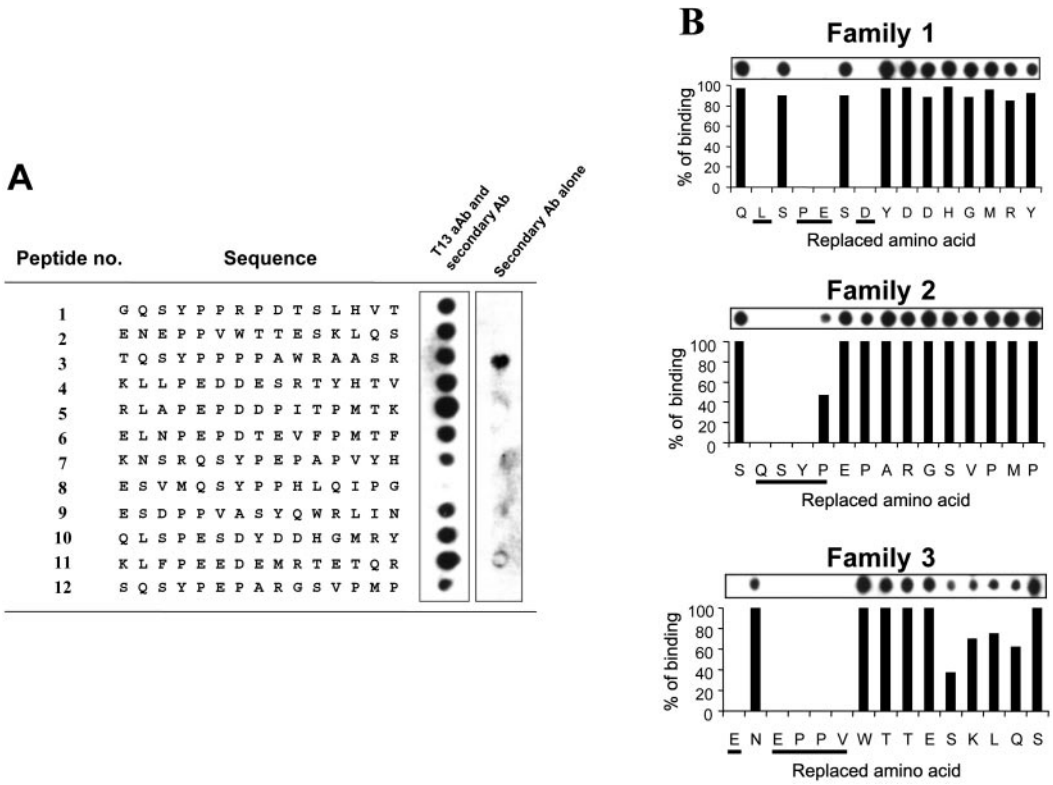

FIG. 2. **Analysis of T13-specific mimotopes by the Spot technology.** *A*, immunoreactivity of peptides with aAb T13 was studied by the Spot technology. aAb T13 reactivity complexed with the secondary antibody and the secondary antibody reactivity alone are shown on the *right* (see "Experimental Procedures"). *B*, identification by alanine scanning of critical residues of mimotopes. A series of alanine analogs of each peptide sequences found previously to be reactive with aAb T13 was prepared and tested by the Spot method. *Replaced amino acid* indicates which residue was replaced by Ala (or Gly when the natural residue is Ala). T13-specific reactivity on the Spot membrane is represented at the *top* of each histogram, and the percent of binding of aAb T13 to each analog compared with the wt sequence is shown by the histograms. Only one representative mimotope for each family is exemplified. *Underlined* amino acids represent the critical residues observed for several peptides stemming from each family.

the X_{15}/f88.4 library were obtained, suggesting that the conformation of 15-mer peptides leads to better recognition by aAb T13. On the other hand, similar experiments performed with another human anti-TPO aAb permitted the selection of peptides from X_{15}/f88.4, X_8CX_8/f88.4, and X_{30}/f88.4 libraries.[3] Except for mimotope RLAPEPDDPITPMTK (Table III), each peptide sequence was obtained individually.

Analysis of T13-specific Mimotopes by Sequence Alignment and Spot Technology—T13-specific mimotopes were aligned with each other and grouped into three families according to their sequence homology (Table IV). Families 1, 2, and 3 contain mimotopes bearing L*X*PE*X*D, (S/T)X_2QSYP*X*P, and EX_2PPVX_6L homologous motifs, respectively (where *X* represents any amino acid). However, peptides KNSRQSYPEPAPVYH, QLSPESDYDDHGMRY, and SQSYPEPARGSVPMP showed similarities found in both families 1 and 2. More generally, the mimotopes often presented a proline-rich sequence representing between 6.6 and 27% of their residues. Acidic amino acids were highly represented in the sequences of Family 1 (between 6.6 and 33% of the residues) and to a lesser extend in Family 3 (between 13.3 and 20% of their residues).

To determine critical amino acids implicated in the recognition of each peptide by aAb T13, we synthesized on a cellulose membrane, by the Spot method, each mimotope followed by an alanine scanning of their amino acid sequences. Most of the 12 mimotopes reacted strongly with the T13 aAb (Fig. 2*A*). Mimotope 8, showing no reactivity with aAb T13, and mimotope 3, demonstrating a cross-reaction with the secondary Ab (Fig. 2*A*), were eliminated from further alanine scanning studies. As exemplified in Fig. 2*B*, the systematic alanine replacement for each mimotope revealed critical residues for T13 binding and identifies three different critical motifs, L*X*PE*X*D, QSYP, and E*X*(E/D)PPV for Families 1, 2, and 3 respectively; these motifs correlated with those demonstrated by sequence homology. Moreover, the alanine scanning patterns clarified the ambiguity for the peptide assignment indicated above, *i.e.* peptides 7 and 12, KNSRQSYPEPAPVYH and SQSYPEPARGSVPMP, were definitively assigned to Family 2, whereas peptide 10, QLSPESDYDDHGMRY, belongs to Family 1 (Table IV).

Localization of Putative T13 Autoantibody Interaction Sites on Human TPO—Amino acid sequences from T13-specific mimotopes were aligned on the primary sequence of hTPO to identify the regions that contain sequence homology on TPO. First, we performed the alignment of critical motifs, identified previously by the Spot technology (Fig. 2*B*), with the primary sequence of hTPO. Then, the other amino acids for each peptide were aligned according to the best homology with the primary sequence of hTPO. As shown in Fig. 3, this procedure identified four different regions (residues 356–382, 713–720, 737–747, and 766–775) which demonstrated the best matching with mimotopes and their critical motifs. Interestingly, two regions bear the amino acids Lys^{713} and Tyr^{772}, described previously as critical for immunodominance (15, 32). Analysis of the three-dimensional model of hTPO showed that these regions are located at the surface of the globular structure (Fig. 4*A*) and could form an immunodominant binding surface (IBS) between the MPO- and CCP-like domains because of the flexibility of the hinge regions (Fig. 4, *A* and *B*). Because these locations correspond to the putative T13 aAb interaction sites on TPO,

[3] D. Bresson, M. Cerutti, G. Devauchelle, S. Bonniol, D. Laune, T. Chardès, and S. Péraldi-Roux, unpublished data.

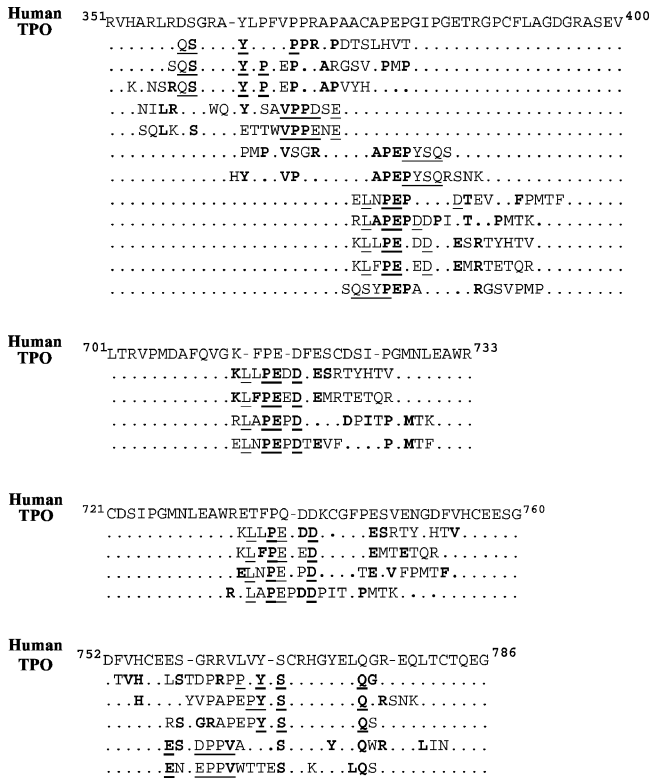

FIG. 3. **Sequence alignment between mimotopes and hTPO sequences.** The alignments were obtained as described under "Experimental Procedures." The critical motifs of T13-specific mimotopes are *underlined*. Identical residues between mimotopes and the primary sequence of hTPO are represented in *bold letters*.

we produced six TPO mutants by overlap extension PCR (Table V) according to sequence alignment. The three-dimensional model revealed that region 356–382 presented two exposed loops around the putative interaction site; thus two distinct TPO mutants, each showing a mutated region on each distinct loop ($TPO^{353–363}$ and $TPO^{377–386}$) were constructed. As control, a TPO mutant, bearing a mutated region (residues 506–514) not identified by mimotope alignment but located close to the IBS (Fig. 4, *A* and *B*), was also generated. All the mutations were performed according to two rules: (i) when different, the amino acids were replaced by those present in the primary sequence of the human MPO for the mutants $TPO^{353–363}$, $TPO^{377–386}$, $TPO^{506–514}$, and $TPO^{713–720}$ or the primary sequence of the CCP domain of the factor H protein for the mutant $TPO^{766–775}$; and (ii) when similar, the residues were present in the TPO/MPO and TPO/factor H sequences, amino acids were replaced by uncharged residues (alanine or leucine). For example the amino acid Arg^{355} was replaced by Ala^{355} in the mutated protein ($TPO^{353–363}$). For the mutant $TPO^{737–740}$, located in the fringe of the MPO and CCP modules, we used only alanine or leucine substitutions. Finally, the Cys^{768} residue was not changed because it could contribute to the overall folding of the TPO molecule by formation of a disulfide bridge in the CCP-like domain.

Expression and Analysis of Wild-type and Mutated TPO—To demonstrate that the mutated regions are a part of the IDR, the wt and the chimeric proteins were expressed in eukaryotic cells by using the new Flp-In™ expression system able to produce a similar level of different proteins of interest. By immunofluorescence, we observed a defect in the transport of the mutant $TPO^{766–775}$ to the plasma membrane (data not shown). A similar observation was described recently by Umeki *et al.* (51), who showed that when the Gly^{771} is replaced by Arg^{771} in

TABLE V
Comparison of the amino acid sequences between wild-type and mutated TPO

Mutant[a]	Wild-type sequence	Mutated sequence
$TPO^{353–363}$	HARLRDSGRAY	NQAFQANGAAL
$TPO^{377–386}$	PEPGIPGETR	LLTNRLGRIG
$TPO^{506–514}$	ASFQEHPDL	NRYLPMEPN
$TPO^{713–720}$	KFPEDFES	SYARLAVN
$TPO^{737–740}$	PQDD	ALAA
$TPO^{766–775}$	YSCRHGYELQ	LTCEGGFRIS

[a] The mutants are indicated by the position of the first and last mutated amino acid in the primary sequence of human TPO.

the TPO genes of patients, this results in a localization defect (accumulation of mutated TPO in the endoplasmic reticulum) and causes congenital hypothyroidism. To overcome this problem, we decided to extract all membrane proteins from wt and stably transfected CHO and to study them by Western blotting and ELISA. All antibodies tested by Western blotting were reactive, under nonreducing conditions, with a protein of ~110 kDa, corresponding to the hTPO (Fig. 5*A*). The polyclonal rabbit antiserum was able to recognize all TPO mutants whatever the conditions. The mutations did not globally affect the expression level for most of the chimeric proteins, even though the expression of mutant $TPO^{737–740}$ was lower than that of the five others. This lower expression was confirmed with all mAb tested. As expected, mAb 47, which recognizes a linear determinant (713–721) (42), did not bind to the mutant $TPO^{713–720}$ but reacted with all of the other mutants under native or denatured conditions. Surprisingly, mAb 6F5, as well as aAb T13, was not reactive under denaturing conditions with wt or mutated TPO (Fig. 5*A*). Furthermore, only the binding of mAb 6F5 to the mutant $TPO^{766–775}$ was eliminated under native conditions. These results demonstrate that mAbs 6F5 and T13 are directed against two different conformational epitopes that overlap in region 766–775. We conclude from these observations that (i) the folding of the TPO mutants is homologous to that of the wt TPO and (ii) in the mutated regions, amino acids 766–775 compose only a part of the conformational epitope recognized by mAb 6F5. Finally, the reactivities of aAb T13 to native proteins are different depending on the mutants. Strong signals were observed with wt TPO and mutant $TPO^{506–514}$, whereas binding of aAb T13 to mutants $TPO^{353–363}$, $TPO^{377–514}$, and $TPO^{766–775}$ was markedly decreased or totally abrogated for mutant $TPO^{713–720}$. To confirm that the epitope of aAb T13 is in both the MPO- and the CCP-like domains, mAbs 47 and 6F5 were used in competition with aAb T13 for the binding to TPO in an ELISA. As shown in Fig. 5*B*, the murine mAbs competed in a dose-dependent manner with aAb T13 and partially inhibited the binding of aAb T13, an inhibition of 45 and 35% for mAb 47 and 6F5, respectively, with a molar excess of 100-fold for the inhibitor. No inhibition was observed with a murine mAb as control. Nevertheless, we could not exclude a steric hindrance by using the competition method, therefore we studied the interaction of mAb 6F5 and aAb T13 with membrane proteins from wt and mutated TPO by ELISA (Fig. 6*A*). Whereas mAb 6F5 recognized similarly the wt and mutant TPO (except for mutant $TPO^{766–775}$), aAb T13 showed a significant and specific binding both to wt TPO and, as expected, to $TPO^{506–514}$. However, the other mutations significantly reduced the T13 aAb binding on TPO. Mutations 353–363, 377–386, and 766–775 partially affected aAb T13 recognition of TPO, whereas amino acid replacements in 713–720 totally abolished the binding of aAb T13 to TPO. These results reinforce the previous observations obtained by Western blotting (Fig. 5*A*).

Analysis of TPO Mutant Recognition by Patient Serum—To

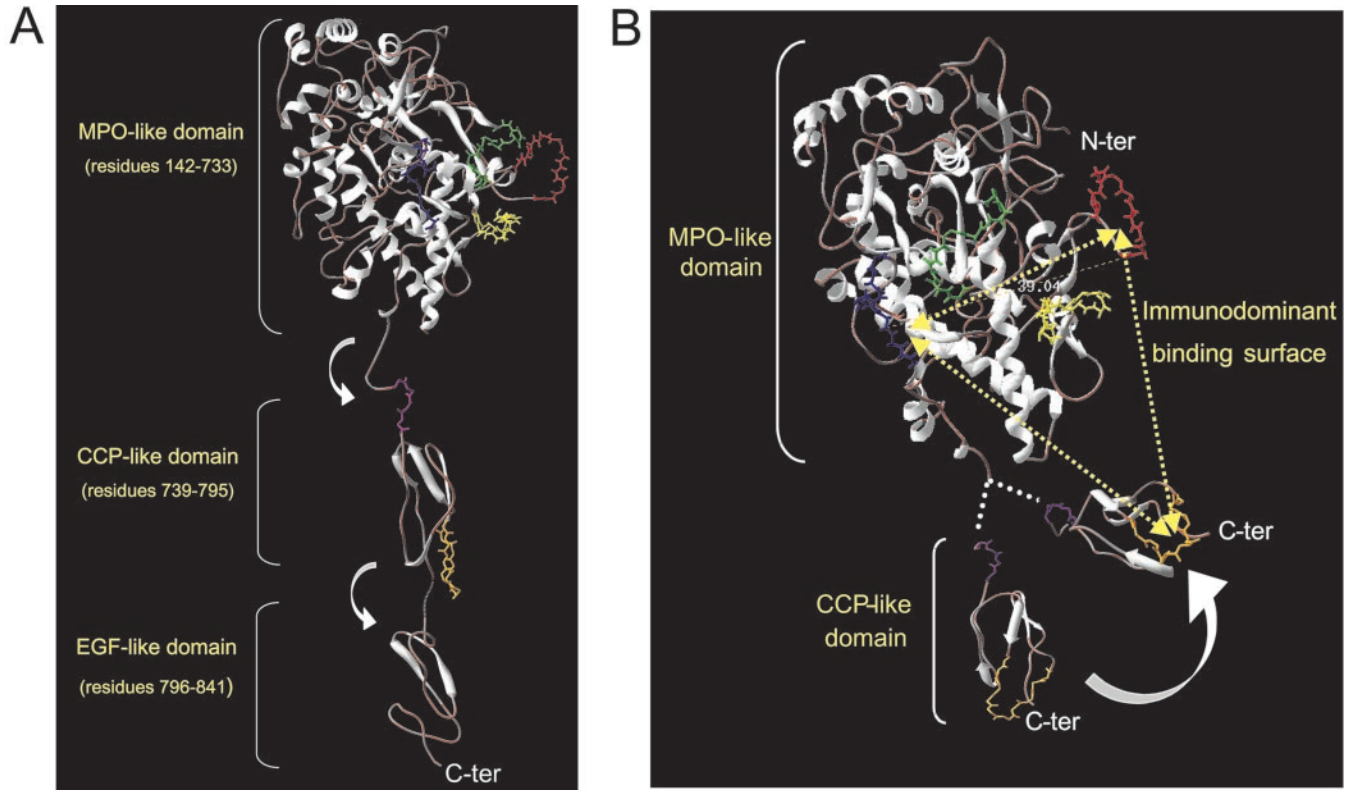

FIG. 4. **Location of the mutated regions on a three-dimensional ribbon diagram of the structure of hTPO.** *A*, ribbon diagram of the structure of hTPO showing the MPO-, CCP-, and EGF-like domains, reproduced with permission (13). This representation corresponds to the juxtaposition of the three-dimensional model of each domain. The mutations produced by "guided" mutagenesis are represented, positions 353–363 in *yellow*, 377–386 in *red*, 506–514 in *green*, 713–720 in *blue*, 737–740 in *pink*, and 766–775 in *orange*. The flexibility of the hinge regions is represented by a *white arrow*. *B*, ribbon diagram representing the possible folding of the CCP-like domain on the MPO-like domain (to simplify the figure, the EGF-like domain is not represented). A *white arrow* indicates the plausible movement of the CCP domain to form the IBS virtually represented by *three yellow dotted lines*. The junction between MPO- and CCP-like domains is shown by *white dotted lines*. The distance (in Å) between the regions 377–387 and 713–720 is shown. The model was adjusted by using Swiss-PDB viewer 3.7b2 freeware available at www.expasy.ch/spdbv.

place this study in a pathological context, the binding of anti-TPO aAbs from sera of patients suffering from AITD, other autoimmune affections, and healthy donors was investigated by ELISA as performed above with mAb 6F5 and aAb T13 (Fig. 6*B*). Whereas the sera from healthy donors or patients suffering from autoimmune pathologies (type 1 diabetes, systemic lupus erythematosus, rheumatoid arthritis, or vasculitis) did not react with any clone (data not shown), all sera from patients with Hashimoto's thyroiditis or Graves' disease specifically bound to wt TPO in a dose-dependent fashion. Control mutations in positions 506–514 did not globally affect the binding of patient serum, whereas mutations in other positions decreased the binding to TPO. Interestingly, these mutants could be classified into two groups, which weakly ($TPO^{377–386}$) or strongly ($TPO^{353–363}$, $TPO^{713–720}$, $TPO^{766–775}$) affected the binding of the anti-TPO aAbs. In contrast to competition studies between anti-TPO mAb and polyclonal patients' sera described previously by our group and others (13, 14, 25, 40, 41), where the results could be biased by steric hindrance, the effects of each mutation on the binding of all polyclonal anti-TPO sera studied here resulted in the same pattern for the particular mutation. Similar results were obtained by McLachlan and Rapoport's group (30).

DISCUSSION

The three-dimensional structure of the hTPO molecule has not been solved by crystallographic studies, even if low resolution diffracting crystals have been obtained (17, 18). However, analysis of the three-dimensional structure of hTPO as assessed by homology modeling denotes a highly complex structure comprising three distinct modules, MPO-, CCP-, and EGF-like domains (13). This highly organized architecture of the TPO autoantigen is a plausible explanation for the anti-TPO aAb reactivity, which is directed mainly to a discontinuous IDR on the native structure of their autoantigen (19, 52). Previous investigations aimed at defining the IDR used rabbit polyclonal antisera directed against TPO polypeptide fragments (13, 24) or murine mAbs (25) in competition with human aAbs. These studies, even if they lead to a better knowledge of the IDR, used Abs produced by animal immunization which do not exactly reflect the hTPO-specific aAb repertoire in AITD. Others studies (33–35), which used eukaryotic cells transfected with MPO-TPO chimeras, did not lead to the structural identification of the IDR, probably because of the low antigen expression of the transfected clones and/or high heterogeneity of TPO expression by the clones. More recently, Guo *et al.* (30) clearly excluded the EGF-like domain as being a part of the IDR and localized this region in the junction between MPO- and CCP-like domains but with a much larger extension in the MPO module. Although these results are crucial to localize globally the IDR, up to now few data have been reported on the identification of restricted regions on these domains recognized by human aAbs and on the location of the IDR in the three-dimensional structure of hTPO.

We hypothesize that phage-displayed peptide technology followed by sequence alignment is presently the most powerful strategy to position discontinuous epitopes on a highly complex structure like hTPO (38, 39, 53). In the present study, we have applied this technology to the well characterized human anti-TPO aAb T13 in an attempt to identify peptides able to mimic

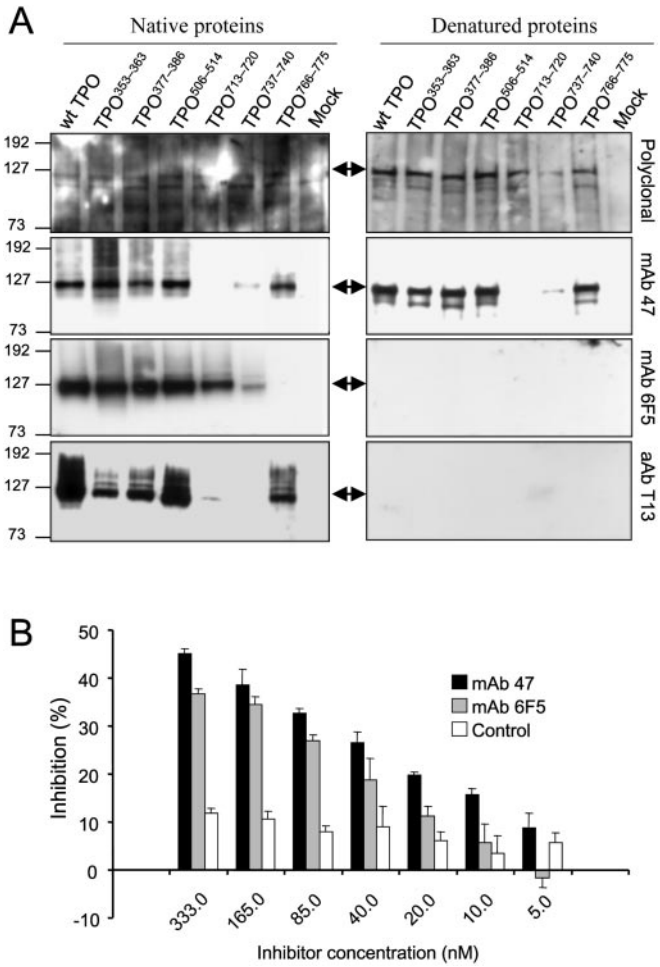

FIG. 5. **Western blotting and ELISA evidence that aAb T13 recognizes both MPO- and CCP-like domain.** *A*, Western blots with native or denatured membrane proteins were performed as indicated under "Experimental Procedures." mAb 47 (10 μg/ml), mAb 6F5 (10 μg/ml), aAb T13 (10 μg/ml), and rabbit polyclonal antiserum (1:300) were used and are identified on the *right* of the figure. TPO-specific bands are shown by *black arrows*, and the molecular masses in kDa are given on the *left*. *B*, competitive ELISA experiments were performed with mAb 47, mAb 6F5, and murine mAb 2C2 against digoxigenin (control) as competitor for the binding of aAb T13 to TPO (see "Experimental Procedures").

its discontinuous and immunodominant epitope. After sequence alignments between critical peptide motifs and the primary sequence of hTPO, we clearly demonstrated by directed mutagenesis on hTPO and generation (with the new Flp-In system) of isogenic stable mammalian cells expressing the same level of wt and mutated TPO that four restricted regions (regions 353–363, 377–386, and 713–720 in the MPO-like domain and region 766–775 in the CCP-like domain of TPO) delineated the IBS on the three-dimensional structure of hTPO. Moreover, by comparison with wt and mutant TPO, aAb T13 and patients' sera showed different binding levels, depending on the mutated region. Whereas mutations in region 377–386 only weakly affected the binding of human aAbs, mutations in regions 353–363, 713–720, and 766–775 strongly reduced their recognition (Fig. 6, *A* and *B*).

These data emphasize the discontinuous nature of the IDR and provide new insights into the MPO- and CCP-like positioning. Indeed, the CCP-like module needs to be close to the MPO-like domain to form the putative interaction surface with the human recombinant aAb T13. As shown in Fig. 4*B*, regions 377–386, 713–720, and 766–775 (constituting the extremities of the IBS) delineate an autoantigenic surface. The antigen/antibody interfacial areas identified for other discontinuous epitopes by x-ray crystallographic analyses and NMR studies have been reported to be between 650 and 1,000 Å^2 (54, 55). Thus, to form an IBS compatible with these areas, the distance between the regions 377–386, 713–720, and 766–775 must be close enough to each other. The structural folding of the three domains constituting the hTPO appears to be homologous with known proteins such as MPO, the CCP module of the factor H, and EGF (13), but no information is presently available concerning the exact folding of one domain in relation to the others. Estienne *et al.* (15) underlined the high flexibility of the hinge region separating the CCP- and EGF-like domains. We hypothesize a similar flexibility between the MPO- and CCP-like domains to form the IBS. Furthermore, we propose two possibilities to explain this phenomenon: either the MPO-like and CCP-like domains interact directly by interactions such as hydrogen bonds or salt links or the flexibility of the hinge region results in constant rearrangement among the three modules, and the binding of an aAb (like T13) on at least two domains "freezes" the structure into a stable conformation. If the latter alternative is true, this could explain why it is so difficult to obtain high resolution diffracting crystals of the TPO ectodomain (17, 18). Co-crystallization of TPO with a specific Fab stabilizing the structure should solve this problem definitively.

Using the phage-displayed peptide technology, we generated peptides recognized by aAb T13 and identified critical motifs (L*X*PE*X*D, QSYP, and E*X*(E/D)PPV) involved in its interaction with these mimotopes. Controversial results have assigned the mAb 47/C21 epitope (713–721) sometimes inside the IDR (25, 32, 56) and sometimes outside this region (23, 35, 57). McLachlan and Rapoport's group (32) deduced from their studies using recombinant antibody TR1.9 that TPO residue Lys^{713}, which is within the human aAb IDR, lies at the fringe of the mouse mAb 47/C21 epitope (32), as is also suggested for the 713–720 region identified by our investigation. Interestingly, other residues from this region such as Pro^{715}, Glu^{716}, and Asp^{717} align with the motif PE*X*D identified in T13-specific mimotopes from Family 1, suggesting that they could contribute to the aAb binding to TPO. Furthermore, the Tyr^{772} residue, recently identified by the Ruf and Carayon's group (15) as critical for immunodominance, is involved in the region 766–775 we characterized as belonging to the IDR. The QSYP motif, identified as critical for aAb T13 binding to mimotopes from Family 2, comprises three residues also found in the 766–775 region of the CCP-like domain. We hypothesize that the QSYP motif mimics a motif composed of residues Tyr^{772} close to Ser^{667}, and Gln^{775} in the three-dimensional TPO structure. These residues could be contact amino acids within the aAb immunodominant epitope. Of interest, the other strongly contributing region, 353–363, also shows residues (Ser^{359}, Tyr^{363}) aligned with the mimotope motif of Family 2 (QSYP) identified by aAb T13. These observations should give us some leads to carry out rational mutagenesis experiments on hTPO and precisely identify the amino acids involved in the IDR, even if we cannot formally exclude that one of these regions contains amino acids essential for the folding of the IDR and is not directly involved in the interaction with aAbs.

Another previously described region, called C2 (16, 58), has been restricted to region 599–617 on TPO and has been defined as one major autoantigenic determinant by inhibition of human anti-TPO aAbs with rabbit polyclonal antisera directed against this peptide (13). Inspection of the three-dimensional TPO model shows that this epitope is located on the opposite side of the MPO-like domain with regard to the IBS we describe here. This observation could be explained by the fact that overlap-

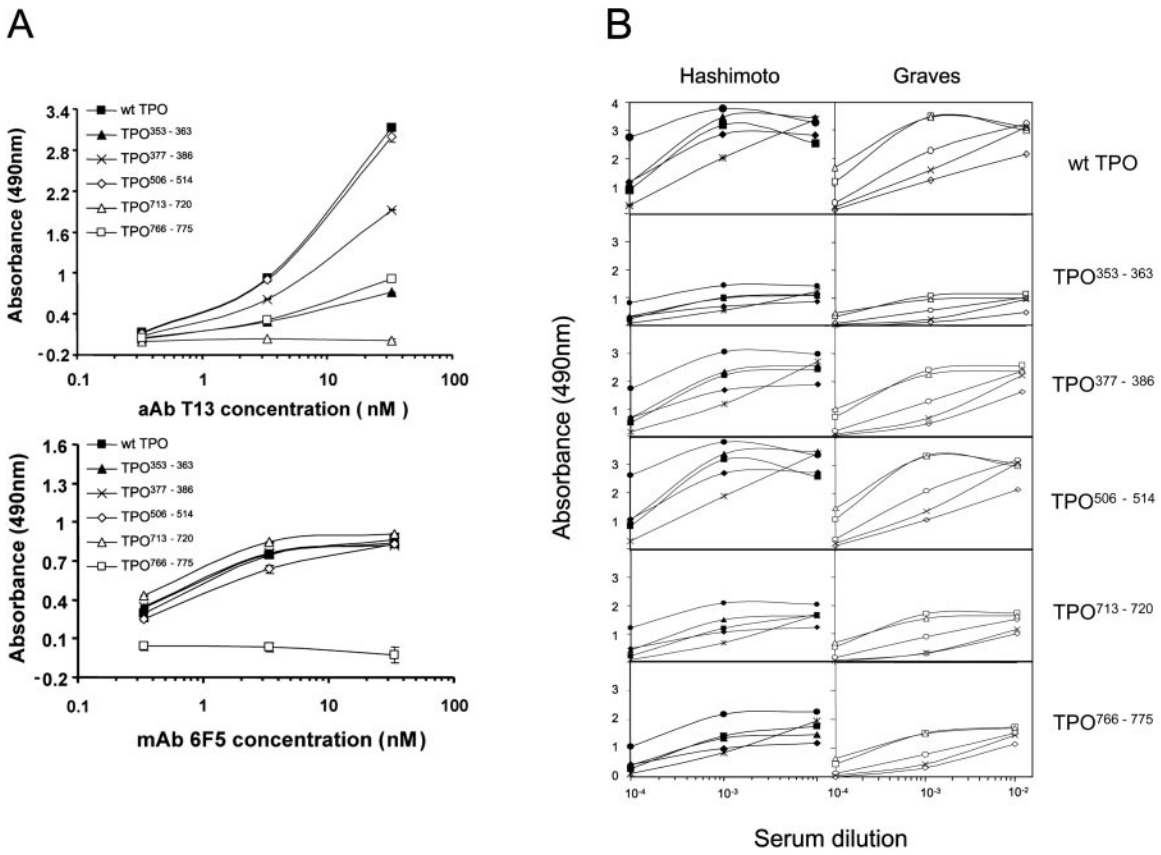

FIG. 6. **The binding of anti-TPO mAb or patients' sera to membrane proteins is affected by TPO mutations.** The effects of TPO mutations on the binding of anti-TPO mAb or patients' sera binding were evaluated by ELISA. *A*, the results obtained with aAb T13 or mAb 6F5 are shown. *B*, patients' sera with Hashimoto's thyroiditis (patient 1 (●), patient 2 (■), patient 3 (▲), patient 4 (♦), and patient 5 (*)) and Graves' disease (patient 6 (○), patient 7 (□), patient 8 (△), patient 9 (◇), and patient 10 (x)) were tested for their ability to bind to the membrane proteins extracted from wt or stably transfected CHO (see "Experimental Procedures"). The results are given in absorbance after subtraction of the background values corresponding to the binding of sera to membrane proteins from nontransfected CHO and are expressed as the mean ± S.D. of duplicate values.

ping antigenic domains have been characterized on the TPO molecule. Particularly, two overlapping immunodominant domains, named A and B (23, 25), have been described based on the competition between polyclonal anti-TPO from patients and human or murine Abs. It is important to note that the A domain defined by the murine mAbs (25) corresponds to the B domain defined by the human Fabs (23) and vice versa. As we used a human anti-TPO aAb in our experiments as did McLachlan and Rapoport's group (23), we chose to use the nomenclature of the IDR/A and B defined by this group. Consequently, the Lys^{713} residue is part of the epitope recognized by the IDR/B-specific antibody TR1.9 (32), and region 713–720 belongs to the immunodominant epitope mapped by aAb T13. Furthermore, mAb 47, which recognizes the IDR/B, competes in part with the human aAb T13 for binding to the TPO molecule (Fig. 5*B*). In addition, non-IGKV1–39 aAbs such as IGLV1–40 aAb T13 have been described to interact with TPO IDR/B, whereas antibodies that use the IGKV1–39 germ line light chain gene have been assigned to IDR/A recognition (23). Taken together, we assume that the human recombinant aAb T13 recognizes the IDR/B on the TPO molecule, even if we cannot formally excluded cross-reaction with the A domain caused by overlapping between IDR/A and B.

In conclusion, by combining phage-displayed peptide technology with mimotope sequence alignment on the TPO molecule, we have precisely identified three regions (353–363, 377–386, and 713–720) belonging to the MPO-like domain and one (766–775) located on the CCP-like domain as being a part of the IDR. We have also localized on the three-dimensional model of hTPO the IBS, which comprises these four regions that are crucial for the binding of human anti-TPO aAbs. This IBS is recognized (i) by the human recombinant aAb T13 obtained with antibody phage-displayed library constructed using TPO-purified B cells from Graves' disease patients (40, 41) and (ii) by anti-TPO aAbs from sera of patients suffering from Hashimoto's and Graves' thyroid diseases. Moreover, our demonstration was obtained by using the full-length TPO autoantigen expressed by eukaryotic cells. Because TPO-specific aAbs from patients' sera are directed against this IDR, such a finding would certainly improve our understanding of TPO recognition by the immune system during AITD. Furthermore, the synthesis of a constrained "mini-TPO," which mimics the IDR we identified, could be of great diagnostic value to detect TPO-specific aAbs. From a therapeutic point of view, the findings presented here should help us to design rational bioactive peptides able to block antigen presentation by B cell membrane-bound TPO-specific aAbs (6, 7), leading to the autoimmune T cell response in AITD and to block the cytotoxic activity of aAbs from patients suffering from AITD, both of these mechanisms resulting in thyroid destruction.

Acknowledgments—We thank Dr. S. L. Salhi for carefully reading the manuscript. We also thank Drs. J. Ruf and P. Carayon for providing the mAb 47; Drs. B. J. Sutton, P. Hobby, and J. P. Banga for permission to use the three-dimensional model of TPO; and Drs. L. Baldet and A. M. Puech for providing patient sera. We acknowledge Dr. N. Chapal for performing scFv T13 characterization, S. Bonniol and Dr. D. Laune for assistance in the cloning of aAb T13, and A. Ozil and M. Ozil for technical assistance with baculovirus expression. We are also grateful

to B. Nguyen for expert technical assistance and S. Villard for the Spot synthesis.

REFERENCES

1. Kaufman, K. D., Rapoport, B., Seto, P., Chazenbalk, G. D., and Magnusson, R. P. (1989) *J. Clin. Invest.* **84,** 394–403
2. Zimmer, K. P., Scheumann, G. F., Bramswig, J., Bocker, W., Harms, E., and Schmid, K. W. (1997) *Histochem. Cell Biol.* **107,** 115–120
3. Taurog, A., Dorris, M. L., and Doerge, D. R. (1996) *Arch. Biochem. Biophys.* **330,** 24–32
4. McLachlan, S. M., and Rapoport, B. (1992) *Endocr. Rev.* **13,** 192–206
5. McLachlan, S. M., and Rapoport, B. (2000) *Int. Rev. Immunol.* **19,** 587–618
6. Guo, J., Quaratino, S., Jaume, J. C., Costante, G., Londei, M., McLachlan, S. M., and Rapoport, B. (1996) *J. Immunol. Methods* **195,** 81–92
7. Guo, J., Wang, Y., Rapoport, B., and McLachlan, S. M. (2000) *Clin. Exp. Immunol.* **119,** 38–46
8. Guo, J., Jaume, J. C., Rapoport, B., and McLachlan, S. M. (1997) *J. Clin. Endocrinol. Metab.* **82,** 925–931
9. Metcalfe, R. A., Oh, Y. S., Stroud, C., Arnold, K., and Weetman, A. P. (1997) *Autoimmunity* **25,** 65–72
10. Parkes, A. B., Othman, S., Hall, R., John, R., Richards, C. J., and Lazarus, J. H. (1994) *J. Clin. Endocrinol. Metab.* **79,** 395–400
11. Rodien, P., Madec, A. M., Ruf, J., Rajas, F., Bornet, H., Carayon, P., and Orgiazzi, J. (1996) *J. Clin. Endocrinol. Metab.* **81,** 2595–2600
12. Chiovato, L., Bassi, P., Santini, F., Mammoli, C., Lapi, P., Carayon, P., and Pinchera, A. (1993) *J. Clin. Endocrinol. Metab.* **77,** 1700–1705
13. Hobby, P., Gardas, A., Radomski, R., McGregor, A. M., Banga, J. P., and Sutton, B. J. (2000) *Endocrinology* **141,** 2018–2026
14. Estienne, V., Blanchet, C., Niccoli-Sire, P., Duthoit, C., Durand-Gorde, J. M., Geourjon, C., Baty, D., Carayon, P., and Ruf, J. (1999) *J. Biol. Chem.* **274,** 35313–35317
15. Estienne, V., Duthoit, C., Blanchin, S., Montserret, R., Durand-Gorde, J. M., Chartier, M., Baty, D., Carayon, P., and Ruf, J. (2002) *Int. Immunol.* **14,** 359–366
16. Arscott, P. L., Koenig, R. J., Kaplan, M. M., Glick, G. D., and Baker, J. R. (1996) *J. Biol. Chem.* **271,** 4966–4973
17. Gardas, A., Sohi, M. K., Sutton, B. J., McGregor, A. M., and Banga, J. P. (1997) *Biochem. Biophys. Res. Commun.* **234,** 366–370
18. Hendry, E., Taylor, G., Ziemnicka, K., Grennan Jones, F., Furmaniak, J., and Rees Smith, B. (1999) *J. Endocrinol.* **160,** R13–R15
19. Portolano, S., Chazenbalk, G. D., Seto, P., Hutchison, J. S., Rapoport, B., and McLachlan, S. M. (1992) *J. Clin. Invest.* **90,** 720–726
20. Finke, R., Seto, P., and Rapoport, B. (1990) *J. Clin. Endocrinol. Metab.* **71,** 53–59
21. Frorath, B., Abney, C. C., Scanarini, M., Berthold, H., Hunt, N., and Northemann, W. (1992) *J. Biochem.* (*Tokyo*) **111,** 633–637
22. Banga, J. P., Barnett, P. S., Ewins, D. L., Page, M. J., and McGregor, A. M. (1990) *Autoimmunity* **6,** 257–268
23. Chazenbalk, G. D., Portolano, S., Russo, D., Hutchison, J. S., Rapoport, B., and McLachlan, S. M. (1993) *J. Clin. Invest.* **92,** 62–74
24. Gardas, A., Watson, P. F., Hobby, P., Smith, A., Weetman, A. P., Sutton, B. J., and Banga, J. P. (2000) *Redox Rep.* **5,** 237–241
25. Ruf, J., Toubert, M. E., Czarnocka, B., Durand-Gorde, J. M., Ferrand, M., and Carayon, P. (1989) *Endocrinology* **125,** 1211–1218
26. Zanelli, E., Henry, M., and Malthiery, Y. (1992) *Clin. Exp. Immunol.* **87,** 80–86
27. Zanelli, E., Henry, M., and Malthiery, Y. (1993) *Cell. Mol. Biol.* (*Noisy-le-grand*) **39,** 491–501
28. Grennan Jones, F., Ziemnicka, K., Sanders, J., Wolstenholme, A., Fiera, R., Furmaniak, J., and Rees Smith, B. (1999) *Autoimmunity* **30,** 157–169
29. Ewins, D. L., Barnett, P. S., Tomlinson, R. W., McGregor, A. M., and Banga, J. P. (1992) *Autoimmunity* **11,** 141–149
30. Guo, J., McLachlan, S. M., and Rapoport, B. (2002) *J. Biol. Chem.* **277,** 40189–40195
31. Estienne, V., Duthoit, C., Vinet, L., Durand-Gorde, J. M., Carayon, P., and Ruf, J. (1998) *J. Biol. Chem.* **273,** 8056–8062
32. Guo, J., Yan, X. M., McLachlan, S. M., and Rapoport, B. (2001) *J. Immunol.* **166,** 1327–1333
33. Nishikawa, T., Nagayama, Y., Seto, P., and Rapoport, B. (1993) *Endocrinology* **133,** 2496–2501
34. Nishikawa, T., Rapoport, B., and McLachlan, S. M. (1994) *J. Clin. Endocrinol. Metab.* **79,** 1648–1654
35. Nishikawa, T., Rapoport, B., and McLachlan, S. M. (1996) *Endocrinology* **137,** 1000–1006
36. Ganglberger, E., Grunberger, K., Sponer, B., Radauer, C., Breiteneder, H., Boltz-Nitulescu, G., Scheiner, O., and Jensen-Jarolim, E. (2000) *FASEB J.* **14,** 2177–2184
37. Hong, S. S., Karayan, L., Tournier, J., Curiel, D. T., and Boulanger, P. A. (1997) *EMBO J.* **16,** 2294–2306
38. del Rincon, I., Zeidel, M., Rey, E., Harley, J. B., James, J. A., Fischbach, M., and Sanz, I. (2000) *J. Immunol.* **165,** 7011–7016
39. Myers, M. A., Davies, J. M., Tong, J. C., Whisstock, J., Scealy, M., Mackay, I. R., and Rowley, M. J. (2000) *J. Immunol.* **165,** 3830–3838
40. Chapal, N., Chardès, T., Bresson, D., Pugnière, M., Mani, J. C., Pau, B., Bouanani, M., and Peraldi-Roux, S. (2001) *Endocrinology* **142,** 4740–4750
41. Bresson, D., Chardès, T., Chapal, N., Bès, C., Cerutti, M., Devauchelle, G., Bouanani, M., Mani, J. C., and Peraldi-Roux, S. (2001) *Hum. Antibodies* **10,** 109–118
42. Finke, R., Seto, P., Ruf, J., Carayon, P., and Rapoport, B. (1991) *J. Clin. Endocrinol. Metab.* **73,** 919–921
43. Poul, M. A., Cerutti, M., Chaabihi, H., Devauchelle, G., Kaczorek, M., and Lefranc, M. P. (1995) *Immunotechnology* **1,** 189–196
44. Poul, M. A., Cerutti, M., Chaabihi, H., Ticchioni, M., Deramoudt, F. X., Bernard, A., Devauchelle, G., Kaczorek, M., and Lefranc, M. P. (1995) *Eur. J. Immunol.* **25,** 2005–2009
45. Bonnycastle, L. L., Mehroke, J. S., Rashed, M., Gong, X., and Scott, J. K. (1996) *J. Mol. Biol.* **258,** 747–762
46. Ferrieres, G., Villard, S., Pugnière, M., Mani, J. C., Navarro-Teulon, I., Rharbaoui, F., Laune, D., Loret, E., Pau, B., and Granier, C. (2000) *Eur. J. Biochem.* **267,** 1819–1829
47. Laune, D., Molina, F., Ferrieres, G., Mani, J. C., Cohen, P., Simon, D., Bernardi, T., Piechaczyk, M., Pau, B., and Granier, C. (1997) *J. Biol. Chem.* **272,** 30937–30944
48. Corpet, F. (1988) *Nucleic Acids Res.* **16,** 10881–10890
49. Ho, S. N., Hunt, H. D., Horton, R. M., Pullen, J. K., and Pease, L. R. (1989) *Gene* (*Amst.*) **77,** 51–59
50. Sanger, F., Nicklen, S., and Coulson, A. R. (1977) *Proc. Natl. Acad. Sci. U. S. A.* **74,** 5463–5467
51. Umeki, K., Kotani, T., Kawano, J. I., Suganuma, T., Yamamoto, I., Aratake, Y., Furujo, M., and Ichiba, Y. (2002) *Eur. J. Endocrinol.* **146,** 491–498
52. Rapoport, B., and McLachlan, S. M. (2001) *J. Clin. Invest.* **108,** 1253–1259
53. Lang, S., Xu, J., Stuart, F., Thomas, R. M., Vrijbloed, J. W., and Robinson, J. A. (2000) *Biochemistry* **39,** 15674–15685
54. Davies, D. R., and Cohen, G. H. (1996) *Proc. Natl. Acad. Sci. U. S. A.* **93,** 7–12
55. Spiegel, P. C., Jr., Jacquemin, M., Saint-Remy, J. M., Stoddard, B. L., and Pratt, K. P. (2001) *Blood* **98,** 13–19
56. Czarnocka, B., Janota-Bzowski, M., McIntosh, R. S., Asghar, M. S., Watson, P. F., Kemp, E. H., Carayon, P., and Weetman, A. P. (1997) *J. Clin. Endocrinol. Metab.* **82,** 2639–2644
57. Chazenbalk, G. D., Costante, G., Portolano, S., McLachlan, S. M., and Rapoport, B. (1993) *J. Clin. Endocrinol. Metab.* **77,** 1715–1718
58. Libert, F., Ludgate, M., Dinsart, C., and Vassart, G. (1991) *J. Clin. Endocrinol. Metab.* **73,** 857–1860